Romanian Reports in Physics, Vol. 64, No. 2, P. 411–425, 2012

CONDENSED MATTER

SIMULATION DETERMINATION OF THE TUNABLE ELECTROMAGNETIC PARAMETERS FOR THE Sc DOPED BaM METAFERRITES IN GHz RANGE

D. IONESCU, I. BOGDAN

"Gh. Asachi" Technical University of Iasi, Department of Telecommunications, Carol I Blvd.11, 700506 Iasi, Romania, E-mail: danaity@yahoo.com, bogdani@etti.tuiasi.ro

Received June 29, 2011

Abstract. For the BaM hexaferrite doped with scandium, the ferromagnetic resonance frequency reduces from ca. 60 to 40 GHz or less, in a controlled manner. The Sc BaM slab, included in a composed metamaterial structure containing also a metallic grid array, ensure negative magnetic permeability of the structure used for microwave and millimeter-wave device applications. The propagation passband where magnetic permeability and electric permittivity are both negative is tunable. By structural simulation with HFSS 13.0 for samples inside a rectangular wave guide (30–60 GHz) we have obtained the parametrical curves for the permeability tensor components in the domain where negative values occur and the passband was determined. The central frequency of the passband increases almost linear with the magnetic polarizing field in the domain of 40.23–43.93 GHz, with a slope of 0.830 GHz / kOe, for bias fields between 3.7 and 8.2 kOe. The passband decreases from 8.03 to 5.40 GHz with a slope of - 0.337 GHz / kOe. For substituting ions contents x varying from 0.2 to 1.8, the passband evolution can be described by a $(1.22 \cdot \exp(-1.54\, x) + \text{ct.})$ law. The largest domain of linear passband variation from ca. 8.23 GHz to 0 corresponds to a slabs thickness variation from 0.4 to 1.28 mm, where the passband disappears and the dielectric character of hexaferrite is predominant.

Key words: doped hexaferrite, negative permeability, control parameters, tunable passband, microwave range.

1. INTRODUCTION

The hexagonal ferrites like BaM, Co_2Y and Co_2Z are materials used for magnetic recording media and high frequency circuits with very good results. The hexagonal *M* type of barium ferrite, BaM, is an important hard magnetic material presenting a large coercive force due to the large magnetic anisotropy of the ferrite. The BaM is recommended as an effective material for microwave and millimeter-wave device applications such as isolators, phase shifters, circulators, and also planar millimeter wave filters and phase shifters based on BaM ferrite thin films.

The material is also suited for tunable negative index material devices (TNIMs) such as delay lines, phase shifters and antennas, due to the frequency tunability and highly frequency dispersive properties, even the large insertion loss are still a problem.

The BaM ferrite films with thicknesses of hundred of nanometers can be synthesized on an amorphous substrate and have the properties required for the data recording at a superhigh density [3, 16]. The films have high internal anisotropy field (H_a of ca. 17 kOe and a nominal saturation induction $4\pi M_s$ of $4 \div 8$ kG) [1, 3] and can be used for manufacturing low-loss devices (*e.g.* mm-wave notch filter [4]) in the 30-100 GHz regime without the need for high external magnetic fields. The hexagonal *c*-axis serves as the easy magnetization direction. Due to the high anisotropy field, the desirable millimeter wave frequency can be achieved, even in the absence of an external biasing magnetic field. Consequently, the low loss self-biased high anisotropy hexagonal ferrite films can be used for a wide range of monolithic microwave integrated circuit (MMIC) magnetic devices.

In this paper the scandium-doped *M*-type barium hexagonal ferrites were studied, of the composition $BaSc_xFe_{12-x}O_{19}$ (with 32 atoms per formula unit), which found their applications at low frequency microwave devices such as isolators and circulators. Other applications in microwave range are available due to the tunable properties of the material.

The high anisotropy field of BaM hexaferrite determines that the operation frequencies to be higher than 30 GHz [6]. The substitution of iron by nonmagnetic trivalent ions allows for lower operating frequencies, even below 10 GHz. The role of the doping ions is to modify the high magnetic anisotropy field, which become adjustable by a proper substitution of the Fe ions in the haxaferrite structure. The doped hexaferrites have a lower saturation magnetization and the coercivity decreases. The ferromagnetic resonance frequency (FMR) becomes tunable from 1–100 GHz.

2. MODELING OF THE METAFERRITE

The scandium doped BaM haxaferrite was analyzed in the frequency range of 30–60 GHz. The structure was reproduced with help of the HFSS (Ansoft) simulation program, considering the interactions between microcomponents and the influence of the applied dc/ac fields [13, 14, 15].

The tested model consists of the composed metamaterial structure including a Sc BaM slab and a copper wires array. The structure was adopted in order to study the frequency domain where the magnetic permeability of the ferrite takes negative values and the possibilities of controlling this domain. The field configuration at slab level was modified by varying different external or internal parameters, like magnetizing field, ferrite slab thickness, substituting ions content, metallic array

dimensional parameters. As a consequence, the electromagnetic parameters (electric permittivity, magnetic permeability) modify accordingly with these variations and the tunable character of the structure was pointed out.

2.1. STRUCTURE DETAILS OF BaM

The structural properties of the Sc doped BaM metaferrite can be studied by analyzing the complex structure of BaM hexaferrite and then the Sc substituted lattice.

The hexagonal ferrites category includes the ferromagnetic compounds of M, Y, W, Z, U and X type. The M type phase ($BaFe_{12}O_{19}$ or $BaO{\cdot}6Fe_2O_3$), represent the magnetoplumbite type of Ba ferrite, with the trade names Ferroxdure and Indox. The crystalline structure of the BaM can be detailed considering that the BaM is isotypic with magnetoplumbite ($PbFe_{12}O_{19}$). The BaM has a hexagonal ferrite complex structure (space group $P6_3/mmc$), with metallic cations distributed among five different sublattices: 12*k*-octahedral, $4f_2$-octahedral, $4f_1$-tetrahedral, 2*b*-tripyramidial, 2*a*-octahedral [5, 7]. The twelve iron ions included in the formula are distributed as follows (Fig. 1): 6/2/1 Fe^{3+} ions occupy the octahedral positions (12*k*, $4f_2$, respectively 2*a*); 2 Fe^{3+} ions occupy tetrahedral sublattice ($4f_1$); one Fe^{3+} ion is placed in a trigonal bipyramid (2*b*) with five fold coordination.

The hexagonal unit cell contains 38 O^{2-} ions, 2 Ba^{2+} ions, and 24 Fe^{3+} ions (a total of 64 ions in a single unit cell). The unit cell was reconstructed with help of the HFSS, considering the backbone structured of the ten O layers and in each fifth layer an O ion substituted with Ba. The Fe^{3+} ion sublattices are completing the frame. The structure can be divided in four blocks (separated in figure 1 by the dash-dot lines): two spinel blocks *S*, interposed by two hexagonal *R* blocks that contains the Ba^{2+} ions [7]. The second *S*, respectively *R* blocks are rotated 180° around the hexagonal axis and denoted with asterix (*). The chemical formula of the *R* and *S* blocks can be written: $R = (Ba^{2+}Fe^{3+}{}_6O^{2-}{}_{11})^{2-}$ and $S = (Fe^{3+}{}_6O^{2-}{}_8)^{2+}$.

Ferrimagnetism is determined by the opposite spin directions of the iron ions in the sublattices. The ion spins configuration is: the Fe^{3+} ions in 12*k*, 2*a*, and 2*b* sublattices have their spins up (16 ions per unit cell), while the Fe^{3+} ions in $4f_1$ and $4f_2$ sites have their spins down (8 ions per unit cell). One obtains a theoretical total moment of 8.5 μ_B = 40 μ_B per unit cell [6]. The superexchange interactions have an antiferromagnetic character. As a consequence, the ordering of spins is collinear ferrimagnetic.

The magnetizing field induced by simulation is a static magnetic field that aligns the magnetic moments along the field direction to minimize its potential energy. The applied RF field inside a rectangular waveguide interacts with the macroscopic metamaterial sample and the *S*-parameters characterizing this interaction are given by the HFSS program, by simulating a proper exposure configuration.

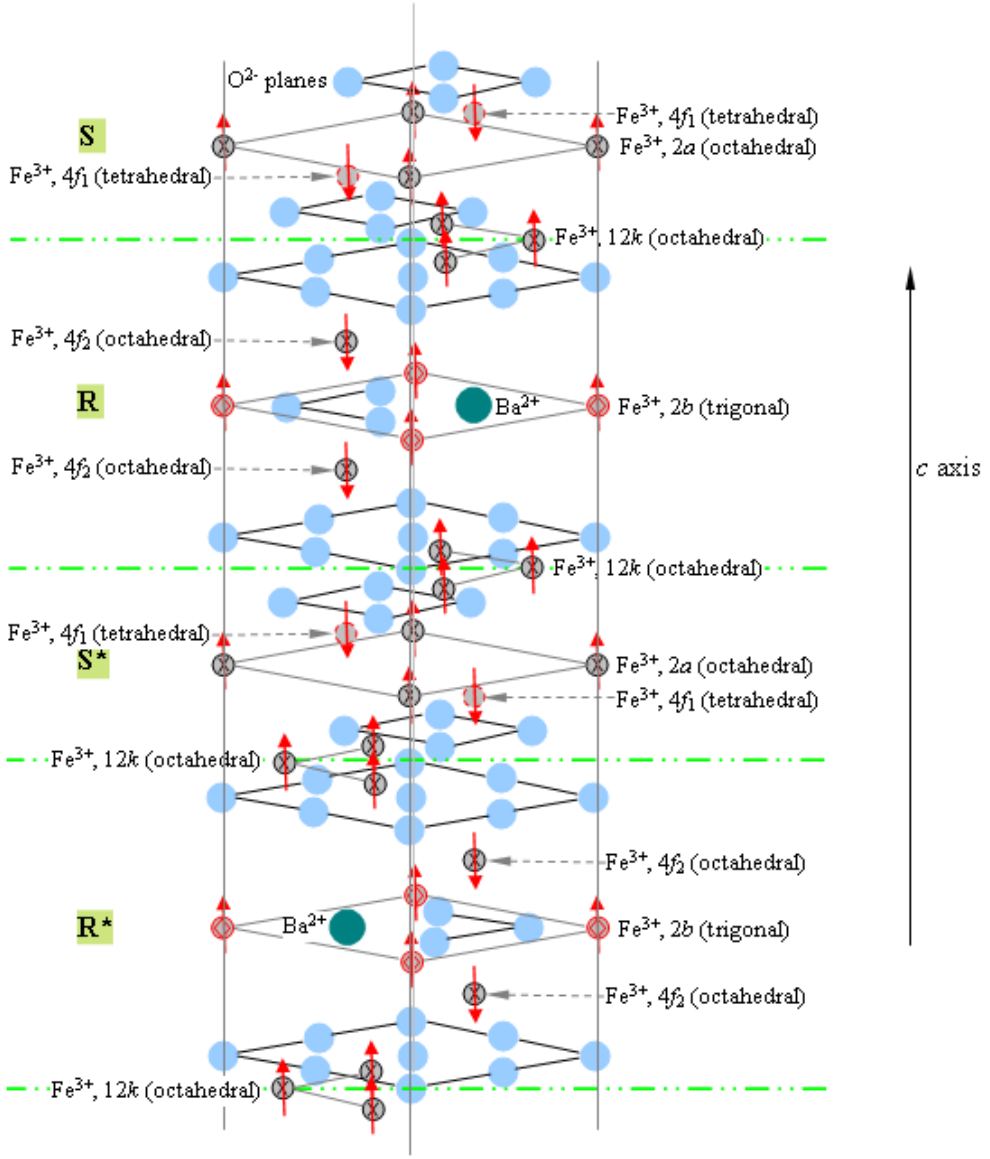

Fig. 1 – The crystallographic structure of BaM hexagonal ferrite. The ten oxygen layers can be observed (the structure backbone) and also the spinel blocks *S* alternating with the hexagonal *R* blocks. The 2*b* trigonal sites are due to the absence of an O^{2-} ion and are firstly occupied by Sc^{3+} ions (then the tetrahedral sites are occupied for higher Sc contents). The spin configuration is also indicated.

The hexagonal crystallographic *c*-axis represents the easy magnetization direction. The hexagonal ferrite present a high uniaxial magnetic anisotropy, which is attributed mainly to the contribution of Fe^{3+} ions placed in trigonal bipyramidal

sublattices 2*b* [7]. The anisotropy field H_a is referred as the magnetic field required for the rotation of magnetization vectors from [001] to [001] directions for *c*-axis anisotropy.

Different substitutions are possible in the BaM type hexagonal ferrite, without introducing any additional atomic structural disorder into the barium hexagonal structure (32 atoms per formula unit, 64 atoms in a single unit cell). As a result, the values of the electromagnetic parameters of the ferrite changes in a large enough domain to become interesting for different microwave applications [6, 17].

The Sc^{3+} ions replace a percent of the Fe^{3+} ions in the crystallographic structure. The Sc-BaM formula can be written like $BaSc_xFe_{12-x}O_{19}$, with *x* coefficient ranging usually from 0 to 1.8. The substitution ions occupy first the bipyramidal site in *R* blocks [6] when the percentage of doping is small ($x < 1$) and then the tetrahedral sites when the doping is harder. The structure details for the single crystalline Sc BaM (the mixed-layer structures, interatomic distances, fractional coordinates of atoms in the asymmetric unit, etc.) were taken from literature [6, 7]. The unit cell parameters were considered of $a = b = 5.8920$ Å, $c = 23.1830$ Å, $\alpha = \beta = 90^0$, $\gamma = 120^0$.

The physical effect of substitution of iron by scandium was found to reduce the anisotropy field and saturation magnetization values [6]. The effect is harder when the Sc concentration increases, but the substitution degree is not recommended to be increased to much (lattice modifications can be induced, indicated also by the structural simulation program). We have to consider that the scandium ion is nonmagnetic, while the Fe^{3+} ion has a $5\mu_B$ magnetic moment. For the Sc doped BaM ferrites the FMR shift in the Q-band, which is the most important fact for applications [6, 10]. If we consider the hexaferrite included in the metamaterial structure, the ferromagnetic resonance can be tuned near 40 GHz or even at lower frequencies when we vary the bias field (3.8 ÷ 7.4 kOe) and the doping coefficient *x* (0.4 ÷ 1.8).

For the metamaterial exposed inside the rectangular waveguide, the sample orientation was chosen so that the magnetizing field $H_=$ (parallel with copper wires) to be transverse on the propagation constant β (Fig. 2). The *c*-axis has to be in the hexaferrite slab plane and, in the same time, the *c*-axis is parallel to the magnetizing field $H_=$.

The permeability tensor for the anisotropic metaferrite can be written as [11]:

$$\hat{\mu} = \mu_0 \cdot \begin{pmatrix} \mu_r & -i\mu_\kappa & 0 \\ i\mu_\kappa & \mu_r & 0 \\ 0 & 0 & 1 \end{pmatrix}, \tag{1}$$

with

$$\mu_r = 1 + \frac{\omega_m \left(\omega_0 - 2\pi \cdot i\alpha_1 f\right)}{\left(\omega_0 - 2\pi \cdot i\alpha_1 f\right)^2 - 4\pi^2 f^2} \tag{2}$$

$$\mu_\kappa = \frac{2\pi\omega_m f}{\left(\omega_0 - 2\pi \cdot i\alpha_1 f\right)^2 - 4\pi^2 f^2}, \tag{3}$$

where α_1 is the damping coefficient ($\alpha_1 \cong 0$ in a single-crystal of hexaferrite), $\omega_0 = \gamma_1 H_0$ is the resonance frequency, γ_1 = the gyromagnetic ratio; H_0 is the sum of the external magnetic field and shape anisotropy field along the *c*-axis ($H_= + H_a$), $\omega_m = \gamma_1 M_s$ is the characteristic frequency, M_s = the saturation magnetization for single-crystal of Sc-BaM.

The components of the permeability tensor, μ_r and μ_κ were computed on the basis of a physical algorithm, written for the exposure configuration of the simulated samples.

For a single crystal of Sc-BaM, the saturation magnetization, $4\pi M_s$, is around 3.3 kG, the anisotropy field, H_a, is of ca. 9 kOe (lower than in the BaM case) and the gyromagnetic ratio γ_1 = 2.8 GHz·kOe^{-1} [5], [6]. The external bias magnetic field was taken in range of 6 ÷ 10 kOe. The FMR frequency can be estimated with Kittel's formula:

$$f_0 \cong \gamma_1 \sqrt{\left(H + H_a\right) \cdot \left(H + H_a + 4\pi M_S\right)}. \tag{4}$$

As a result of the resonant interaction between the metaferrite and the field, an abrupt variation of the magnetic properties occurs, illustrated by the HFSS program. The continuity of the curves for the electromagnetic parameters (permittivity, permeability) of the samples near the resonance demonstrates the viability of the method.

2.2. TUNABLE PROPERTIES OF DOPED BaM

In the composed metamaterial structure consisting of the hexaferrite slab with thickness less than a millimeter and the metallic array with copper wires of hundreds of micrometers, the ferrite material is responsible for the negative μ, while the metallic array ensures the negative ε values. On frequency scale, the domain of negative permittivity values is placed near the FMR and overlap partially the domain of negative permittivity values generated by the copper wires. The passband where both ε and μ are negative is tunable by modifying both domains.

The frequency domain where negative permeability occurs can be modified by varying an external or internal parameter, like the magnetic bias field or the ferrite volume factor. By our simulation method parametrical curves where obtained to illustrate the tuning control.

The tunable passband indicates the occurrence of negative refraction index n for the composed metamaterial structure. The main advantage of the structure can be considered the frequency tunability of the passband. Previous studies report a central frequency shift from 40.9 to 43.9 GHz with $H_{=}$ changing from 4.0 to 7.0 kOe [5, 6]. We have obtained similar results by simulation by varying the bias field from 3.8 to 9.2 kOe. The central frequency shifting is almost linear and decreases abruptly for bias field values out of the domain.

The passband is also tunable by varying the hexaferrite slab thickness. Variations from 0.3 mm to 1.3 mm thick of the Sc-BaM slabs were considered in literature, a thinner slab corresponding to a more tunable passband [5, 6]. The effect is dependent on a threshold value of the slab thickness, which was found in our simulations considering the dielectric properties of the hexaferrite. If the hexaferrite slab is thicker than the threshold value the passband disappears and the composed metamaterial present positive permittivity.

A hexaferrite material included in a composed metamaterial structure ensures the frequency tunability of the metamaterial properties, either the metamaterial is a split ring resonator, a transmission line structure or metamaterial with ferrite slab and metallic array. The bandwidth depends strongly of the metamaterial structure [4, 9]. Our simulation investigations gave us the opportunity to determine a continuous variation of the tunable parameters of the material sample over the whole range of frequency domain where tunability occurs and also to determine the threshold values.

3. RESULTS FOR THE NEGATIVE PARAMETERS

Composed metamaterial samples were simulated using two test configurations, in the frequency range of 30–60 GHz. The obtained results verify the known properties of the Sc BaM hexaferrite (large resistivity, high permeability in GHz range) and complete the data for the frequency domains where measurement results are incomplete. The simulation profile was conceived taking into account that the material present a large magnetocrystalline anisotropy, a high Curie temperature, a large saturation magnetization and low dielectric losses ($\tan \delta_e = 0.0002$) [2, 6, 12].

The first test configuration consists of composed metamaterial samples placed inside a rectangular waveguide (with the cross-section 22.86 × 10.16 mm), working on the TE mode. The Sc-BaM slab thicknesses were of 200 to 1 200 μm. The bias field and easy axis of the hexaferrite are both in the slab plane, also parallel with copper wires of the metallic grid array (Fig. 2).

The width of copper wires was taken of 0.2 mm (the thinner wires, the better field modulation can be achieved at metamaterial level) with spacing of 1 mm between wire centers.

A second test configuration was considered for the results confirmation. The hexaferrite slab of the metamaterial samples was simulated on gadolinium gallium garnet substrate (GGG, or the cubic $Gd_3Ga_5O_{12}$), under a horn antenna. Due to the substrate nature no intermediate layers are necessary. The hexaferrite slabs were of 100 to 600 μm.

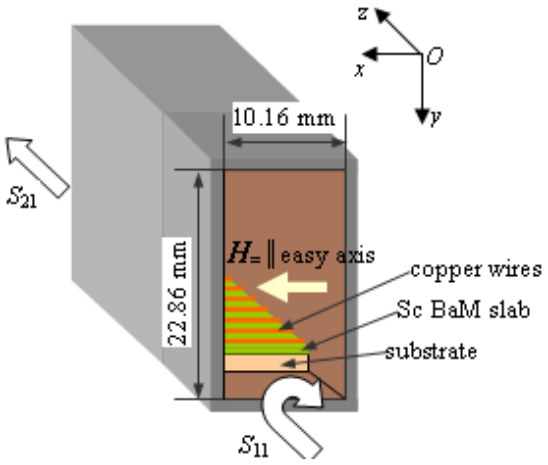

Fig. 2 – The waveguide filled with the metamaterial sample.

The HFSS program gives us the *S*-parameters corresponding to the field propagation through the waveguide with samples. The real, respectively imaginary parts of the relative permeability were calculated, for different values of the magnetic field applied for magnetization. The following expression can be written for the permeability tensor components [10, 11]:

$$\frac{B_{\approx}}{H_{\approx}} = \begin{vmatrix} \mu & -i\kappa \\ i\kappa & \mu \end{vmatrix} = |\hat{\mu}| = \mu_0 \cdot \begin{vmatrix} \mu_r & -i\mu_\kappa & 0 \\ i\mu_\kappa & \mu_r & 0 \\ 0 & 0 & 1 \end{vmatrix} \tag{5}$$

$$\mu = \mu' + i\mu''; \quad \kappa = \kappa' + i\kappa''. \tag{6}$$

Curves which describe the permeability tensor components evolution with frequency modify in function of bias magnetic field, ferrite slab thickness, substituting ions content, metallic array configuration. The first set of parametrical curves was given in Figs. 3, 4 and describe the curves shifting with the bias field, $H_{=}$. The represented area was chosen at frequencies higher to the ferromagnetic resonance, but starting from its vicinity, which is the operating domain of interest in practice.

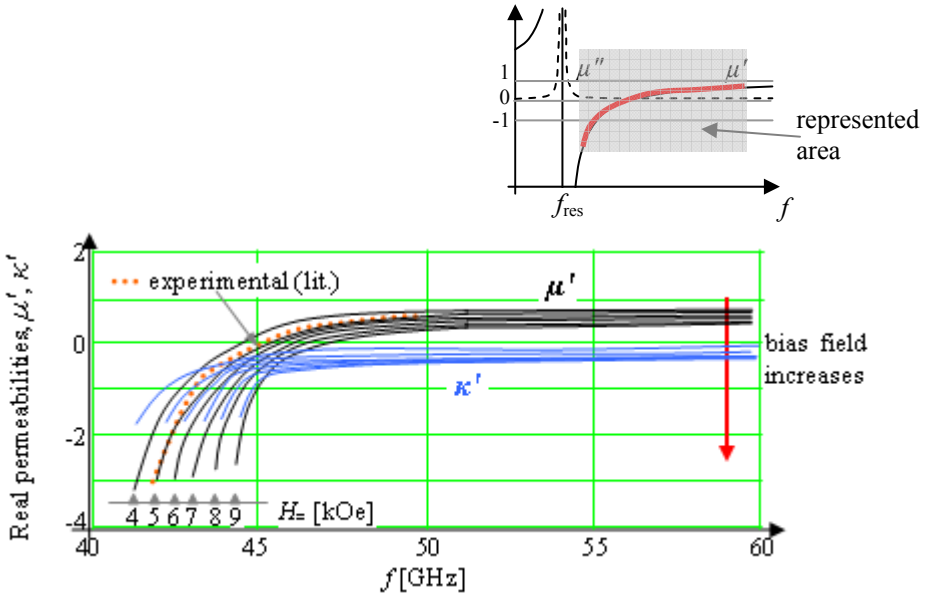

Fig. 3 – Real parts of the permeability tensor components, μ', respectively κ', *versus* frequency, obtained by simulation for the metamaterial with a slab of 0.4 mm of $BaSc_{0.2}Fe_{11.8}O_{19}$. Curves shifting were illustrated on graph when the magnetizing field $H_=$ increases. Curve obtained by measurements at 5 kOe [He &, 2009] was indicated on graph for comparison (orange dot curve). Horizontal short scale indicates the corresponding $H_=$ value for each μ' curve. For the κ' curves, the $H_=$ fields order is similar.

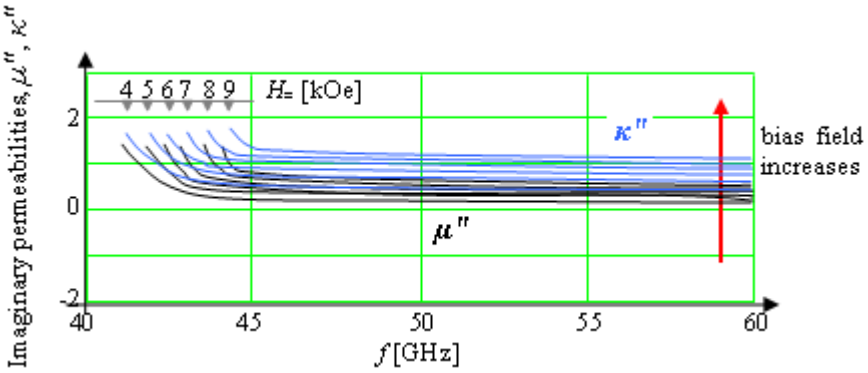

Fig. 4 – Imaginary parts of the permeability tensor components, μ", respectively κ", *versus* frequency, obtained by simulation for the metamaterial with a slab of 0.4 mm of $BaSc_{0.2}Fe_{11.8}O_{19}$. Curves shifting were illustrated on graph when the magnetizing field $H_=$ increases. Horizontal short scale indicates the corresponding $H_=$ value for each κ" curve. For the μ" curves, the $H_=$ fields order is similar.

One observes that curves are shifting almost linear with the bias field magnitude. Constant magnetic polarizing field were considered in the range of 3.8 to 9.2 kOe. For higher polarizing fields, secondary effects occur inside the material

and the corresponding spent energy justifies no more. The bias field variation determines also the permeability magnitude and resonance position modification.

Modification of the curves giving the permeability tensor components *versus* frequency in function of the substituting ions content are illustrated in Fig. 5. A variation of x factor from 0 to 1.8 was considered in the $BaSc_xFe_{12-x}O_{19}$ mixed hexaferrite. One remarks the permeabilities decreasing when the substitution degree increases, due to the weaker magnetization of the sample (Sc ions are nonmagnetic). Curves shifting is an nonlinear effect in this case. Ferromagnetic resonance position modifies not significant.

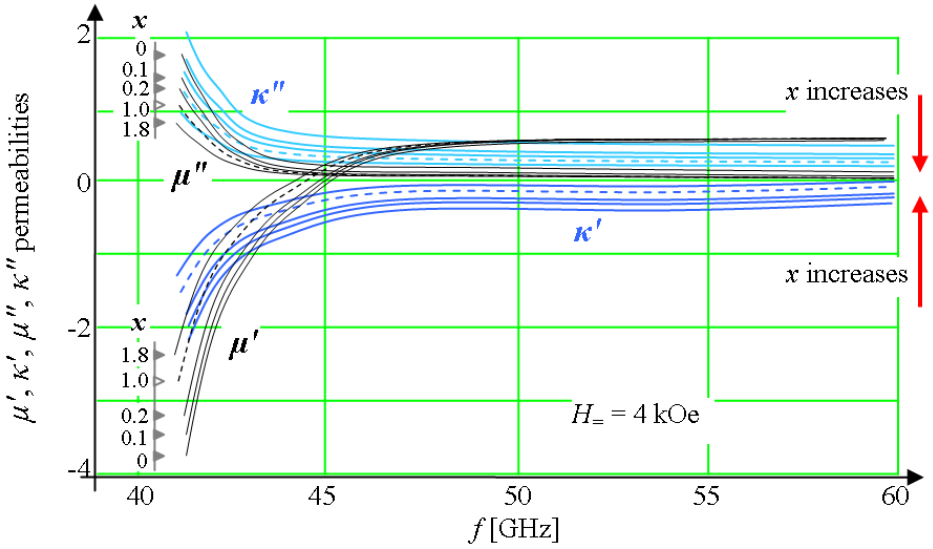

Fig. 5 – Evolution of the curves for the permeability tensor components, μ', κ', μ'', κ'' *versus* frequency, for a variable content of substituting ions, x, obtained by simulation (hexaferrite slab of 0.4 mm). For clarity, curves were represented for a group of selected increasing values of x. Vertical short scales indicate the corresponding x value for each μ' curve (below), respectively for each μ'' curve (above). For the κ', respectively κ'' curves the x parameters order is similar.

The ferrite slab thickness, d, is a parameter which determines a threshold evolution of the propagation passband, where both permittivity and permeability of the composed metamaterial are negative. Due to the metallic array with wires of 0.2 mm or thicker, the hexaferrite slab has to be taken at least with the same thick. Consequently, the considered domain for d was of 0.2 mm ÷ 1.2 mm (Fig. 6).

One observes that the ferromagnetic resonance position on frequency scale remain the same when the hexaferrite slab is thicker (field interact with the same structure), but the domain of negative permeability region becomes more narrow until disappears completely.

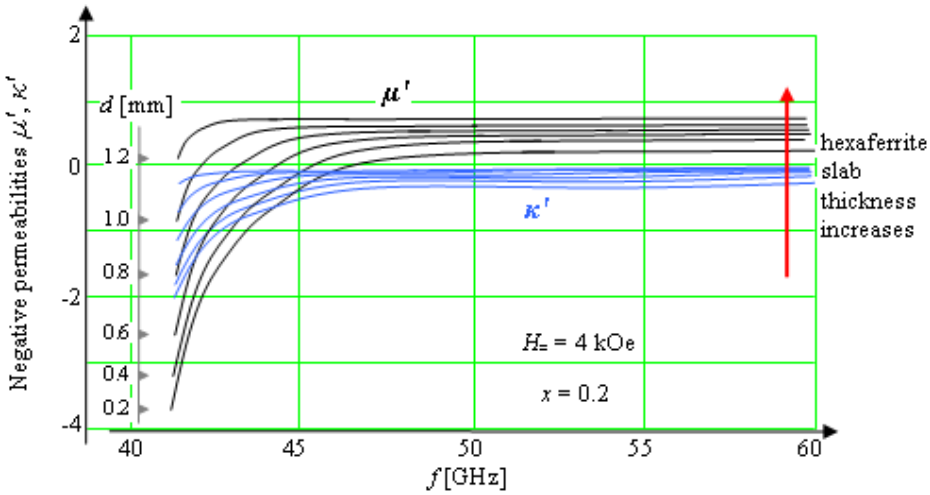

Fig. 6 – Evolution of the curves for the negative components of the permeability tensor, μ', κ', *versus* frequency, when the hexaferrite slab thickness, *d*, increases, obtained by simulation. The domain of the negative values for the μ' restrains and finally disappears when the hexaferrite slabs thickness increases. Vertical short scale indicates the corresponding *d* value for each μ' curve. For the κ' curves the *d* parameters order is similar.

Curves for the permeability tensor components shift when the dimensional parameters of the metallic array are varied, due to the modifications of the field configuration at metamaterial samples level. Copper wire spacing/width and also the distance between the metallic array plane and hexaferrite slab can be varied.

These geometrical modifications do not determine shifting of the ferromagnetic resonance, but the magnitude of the permeability and permittivity peaks are modulated strongly nonlinear. Modification of the geometrical parameters act correlate upon permeability and permittivity pattern for the composed metamaterial and the matter is still in study. As a consequence, the domain where these quantities are negative changes, and implicitly changes the propagation passband.

All the control parameters influence the frequency domain where negative permeability occurs and implicit the propagation passband. Selective results obtained by simulation for the passband and its central frequency are presented in Table 1. The results indicate the character of the passband modification in function of a control parameter, when the other parameters are maintained constant.

An increasing of the magnetic polarizing field determines a consistent shifting of the central frequency of the passband, but the passband decreases (the permeability curves become more abrupt and the domain of negative permeability value become narrower in this case (Fig. 7).

Table 1

Shifting of the central frequency of the passsband and passband value for different sets of control parameters

$H_=$ [kOe]	x	d [mm]	f_c [GHz]	Δf [GHz]	Observations
4	0.2	0.4	40.75	8.03	– bias magnetic field $H_=$ varies – content of substituting ions, x = constant – hexaferrite slab thickness, d = constant
5	0.2	0.4	41.68	7.55	
6	0.2	0.4	42.47	6.92	
7	0.2	0.4	43.22	6.35	
8	0.2	0.4	43.76	5.56	
9	0.2	0.4	44.08	4.32	
4	0	0.4	41.97	5.25	– bias magnetic field $H_=$ = constant – content of substituting ions, x varies – hexaferrite slab thickness, d = constant
4	0.1	0.4	41.95	4.84	
4	0.2	0.4	41.92	4.41	
4	0.6	0.4	41.84	4.06	
4	1.0	0.4	41.37	3.85	
4	1.8	0.4	41.32	3.62	
4	0.2	0.2	41.13	12.43	– bias magnetic field $H_=$ = constant – content of substituting ions, x = constant – hexaferrite slab thickness, d varies
4	0.2	0.4	41.18	8.23	
4	0.2	0.6	41.21	6.02	
4	0.2	0.8	41.23	4.12	
4	0.2	1.0	41.25	2.04	
4	0.2	1.2	41.28	0.06	

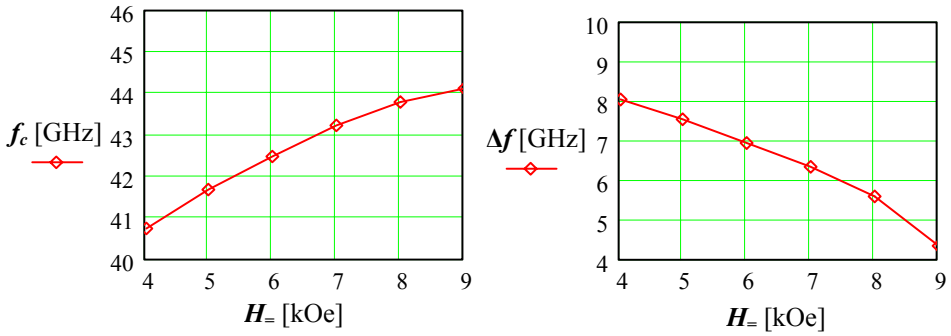

Fig. 7 – Evolution of the central frequency of the propagation passband with the magnetic polarizing field $H_=$ (left graph) and dependence of the passband of $H_=$ (right graph).

The central frequency of the passband presents a low decreasing with the content of substituting ions x, more accentuate for x values in the range of 0.3–0.9 and is almost not sensible at x variations for lower x and for x higher than 0.9 (at the ends of the considered domain). The substitution ions do not influence significantly the structure and implicit the ferromagnetic resonance, but have a certain influence on magnetization degree of the hexaferrite, modifying the shape of the permeability curves. Consequently the passband modifies and a passband decreasing occurs, given in Fig. 8.

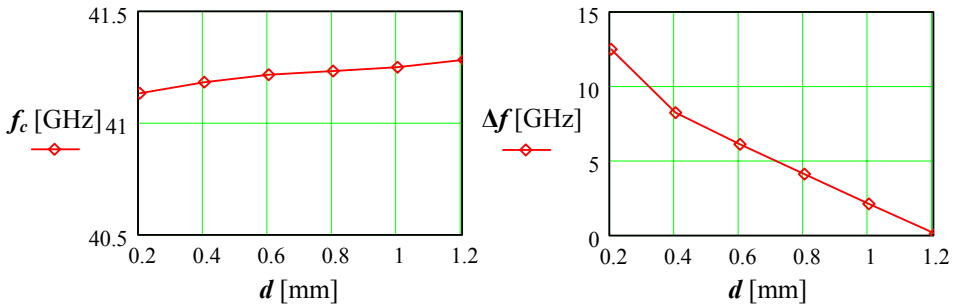

Fig. 8 – Evolution of the central frequency of the propagation passband with the content of substituting ions x (left graph) and dependence of the passband of x (right graph).

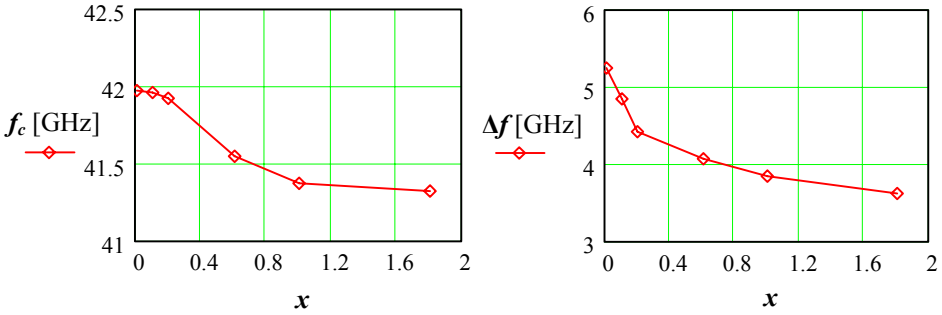

Fig. 9 – Evolution of the central frequency of the propagation passband with the hexaferrite slab thickness, d (left graph) and dependence of the passband of d (right graph).

The hexaferrite slab thickness represents a convenient control parameter for tuning the passband because its central frequency remains practically unmodified (Fig. 9).

An important fact which has to be considered is that the propagation passband disappears for hexaferrite slab thicknesses grater than a threshold value (we found 1.28 mm)), the phenomena inside the material samples modifies and also the interaction character with the exciting microwave field. Due to the hexaferrite nature, the price paid for obtaining the desirable negative permeability is the manifestation of the hexaferrite dielectric character. For thicker slabs, dielectric properties overcome the magnetic character of the hexaferrite (which has an undesirable high dielectric constant), when we consider the interaction field-substance.

Our simulation method is a flexible one due to the fact that a continuous variation of the internal and external parameters is possible for studying their influence on the quantities of interest. The aim of the material studies performed by simulation is the determination of the optimal control parameters for the

modification of samples properties. The obtained evolutional curves are used as a pattern for the tuning process and give us the dependence coefficients between the quantities of interest and the control parameters.

4. FINAL CONCLUSIONS

Mixed metamaterials based on hexaferrite films and a metallic grid array present advantages due to the tunable character of the structure. The electromagnetic properties of the material samples can be controlled by varying an internal or external parameter. The frequency domain where negative permeability occurs and the propagation passband are tunable by changing the magnetizing field of the hexaferrite or the ferrite slab thickness, substituting ions content, metallic array dimensional parameters.

Values of the dependence coefficients between the quantities of interest and the control parameters can be obtained from the parametrical curves obtained by structural simulation. A few domains of interest are pointed out in the following considerations.

The central frequency of the passband increases almost linear with the magnetic polarizing field of the hexaferrite in the domain of 40.23–43.93 GHz, with a slope of 0.830 GHz / kOe, for bias fields between 3.7 and 8.2 kOe. The passband decreases almost linear from 8.03 to 5.40 GHz with a slope of –0.337 GHz / kOe, for bias fields between 8.3 and 4 GHz. Out of these ranges the values of the dependence coefficients can be read for every point on graphs.

The passband evolution for variable substituting ions content can be approximated exponential in the range of 4.34–3.62 GHz, for substituting ions contents of 0.2 to 1.8. A dependence law like $1.22 \cdot (e^{-1.54\,x}) + \text{ct.}$ can be written for the mentioned domain.

The largest domain of passband variation is obtained by modifying the hexaferrite slab thickness. The passband decreases after a polynomial law from 12.43 to ca. 8.23 GHz for slab thicknesses increasing from 0.2 to 0.4 mm. The passband decreasing becomes linear for slabs of 0.4–1.28 mm, where the passband disappears and the dielectric character of hexaferrite is predominant. The linear decreasing slope is of –10.287 GHz / mm.

We can conclude that, by doping with Sc the BaM hexaferrite, one obtains a lower ferromagnetic resonance, moving the application frequency range from U and V bands to Q band.

The metamaterial structure including the Sc BaM hexaferrite and a metallic grid array has tunable propagation passband and possibilities of shifting its central frequency by varying a control parameter, in a relative large domain and following a simple law.

Acknowledgements. This paper was supported by the project PERFORM-ERA "Postdoctoral Performance for Integration in the European Research Area" (ID-57649), financed by the European Social Fund and the Romanian Government.

REFERENCES

1. S. Sugimoto, K. Haga, T. Kagotani, K. Inomata, *Microwave absorption properties of Ba M-type ferrite prepared by a modified coprecipitation method*, J. Magn. Magn. Mater., **290–291**, Part 2, 1188-1191 (2005); Proc. of the Joint European Magnetic Symposia (JEMS' 04).
2. H.-I. Hsiang, R.-Q. Yao, *Hexagonal ferrite powder synthesis using chemical coprecipitation*, Mater. Chem. Phys., **104**, 1–4 (2007).
3. C. Zhao, T. Wang, *Flux growth and magnetic properties of hexagonal ferrite single crystal*, J. Appl. Phys., **61**, 4154–4154 (2009).
4. L. Lu, Y.-Y. Song, J. Bevivino, M. Wu, *Planar Millimeter Wave Notch Filters Based on Magnetostatic Wave Resonance in Barium Hexagonal Ferrite Thin Films*, American Physical Society, Annual Meeting of the Four Corners Section of the APS, October 15–16, 2010, Abstract **#C2.005**; http://adsabs.harvard.edu/abs/2010APS..4CF.C2005L
5. T. M. Meaz, C. Bender Koch, *X-ray diffraction and Mössbauer Spectroscopic Study of* $BaCo_{0.5x}Zn_{0.5x}Ti_x\ Fe_{12-2x}O_{19}$ *(M-type hexagonal ferrite)*, Egypt. J. Sol., **26**, 197–203 (2003).
6. A. Yang, Y. Chen, Z. Chen, C. Vittoria, V. G. Harris, *Magnetic and atomic structure parameters of Sc-doped barium hexagonal ferrites*, J. Appl. Phys., **103**, 07E511 (2008).
7. W. D. Townes, J. H. Fang, A. J. Perrotta, *The crystal structure and refinement of ferrimagnetic barium ferrite,* $BaFe_{12}0_{19}$, Zeitschrift für Kristallographie, **125**, 437–449 (1967).
8. Y. Kitagawa, Y. Hiraoka, T. Honda, T. Ishikura, H. Nakamura, T. Kimura, *Low-field magnetoelectric effect at room temperature*, Nat. Mater., **9**, 797–802 (2010).
9. F. J. Rachford, D. N. Armstead, V. G. Harris, C. Vittoria, *Simulations of Ferrite-Dielectric-Wire Composite Negative Index Materials*, Phys. Rev. Lett., **99**, 057202 (2007).
10. V. G. Harris, A. Geiler, Y. Chen, S. D. Yoon, M. Wu, A. Yang, Z. Chen, P. He, P. V. Parimi, X. Zuo, C. E. Patton, M. Abe, O. Acher, C. Vittoria, *Recent advances in processing and applications of microwave ferrites*, J. Magn. Magn. Mater., **321**, 2035–2047 (2009).
11. R. Marqués, F. Martin, M. Sorolla, *Metamaterials with Negative Parameters, Theory, Design, and Microwave Applications*, John Wiley & Sons, 2008.
12. A. Lupei, V. Lupei, C. Gheorghe, A. Ikesue, *Spectroscopic investigation of* Sm^{3+} *in YAG ceramic*, Rom. Rep. Phys., **63**, 817–822 (2011).
13. N. Negoita, E.A. Patroi, C.V. Onica, *Simulations on dilute magnetic semiconductor properties*, Rom. Rep. Phys., **62**, 115–120 (2010).
14. D. Ionescu, I. B. Ciobanu, *Study in microwave range of some HF board materials for lead-free technologies*, Rom. Rep. Phys., **61**, 676–688 (2009).
15. I. B. Ciobanu, D. Ionescu, *HF Modeling for the Electrical Properties Determination of a Lead-Free Potential Piezoelectric Material*, Rom. Rep. Phys., **61**, 105–114 (2009).
16. I. Jepu, C. Porosnicu, I. Mustata, C. P. Lungu, V. Kunkser, M. Osiac, G. Iacobescu, V. Ionescu, T. Tudor, *Simultaneously thermionic vacuum arc discharges in obtaining ferromagnetic thin films*, Rom. Rep. Phys., **63**, 804–816 (2011).
17. M.-L. Craus, N. Cornei, M. Lozovan, C. Mita, V. Dobrea, *Influence of Na and Cr substitutions on electronic phase diagram of* $La_{0.54}Ho_{0.11}Ca_{1-x}Na_xMn_{1-y}Cr_yO3$ *manganites,* Rom. Rep. Phys., **62**, 780–790 (2010).